Results from Beam Energy Scan Program at RHIC-STAR

ShinIchi Esumi, for the STAR collaboration[a,*]

[a]*Tomonaga Center for the History of Universe (TCHoU),*
Division of Physics, Faculty of Pure and Applied Sciences, University of Tsukuba,
Tenno-dai 1-1-1, Tsukuba, Ibaraki 305-8571, Japan

E-mail: esumi.shinichi.gn@u.tsukuba.ac.jp

Nuclear matter at extremely high temperature and high density is expected to undergo a phase transition to a different state of matter, that is made of deconfined quarks and gluons, such as Quark Gluon Plasma (QGP). The QGP is believed to have existed in early universe just after the Big Bang and/or inside neutron stars. High energy heavy-ion collisions have been carried out in various experiments at AGS, SPS, RHIC and LHC accelerator facilities at Brookhaven National Laboratory (BNL) and European Organization for Nuclear Research (CERN) to create and explore such new state of matter. The experimental results at the highest possible energy regions at RHIC and LHC indicate that the new state of matter has indeed been formed with a partonic degree of freedom, and the phase transition seems to be a smooth crossover that is also expected from the theoretical calculations in the high temperature region of the Quantum Chromo Dynamics (QCD) phase diagram. In the high density area of the QCD phase diagram, the transition is expected to be a first order phase transition and there could be a critical end point for the first order phase transition. The high density region can be reached by lowering the beam energy to a few GeV to a few 10 GeV. Experimental studies with heavy-ion collisions aiming at this high density region are currently being pursued at SPS and RHIC. Future facilities at FAIR, NICA, HIAF and J-PARC are planned. The STAR experiment has been extensively working on the beam energy scan program at RHIC especially around this beam energy region in order to find the first order phase transition as well as signatures from the critical end point in the QCD phase diagram. The recent experimental results of STAR collaboration from the RHIC beam energy scan program will be presented and discussed in this proceedings.

*Speaker

1. Introduction

In order to investigate the property of the new state of nuclear matter at high temperature and high density, four major experiments started taking data at Relativistic Heavy-Ion Collider (RHIC) in 2000. The Solenoidal Tracker At RHIC (STAR) detector, which is one of the biggest experiments at RHIC, consists of a large acceptance cylindrical Time Projection Chamber (TPC) to measure charged particles' trajectories and to perform particle identification at mid-rapidity. Two main findings at RHIC: (1) collectivity during the partonic stage, that has been observed as large elliptic flow of various hadrons, and (2) partonic energy loss, that has been seen as strong suppression of high p_T hadrons, enable the RHIC physicists to declare the discovery of a strongly interacting Quark Gluon Plasma in relativistic heavy-ion collisions.
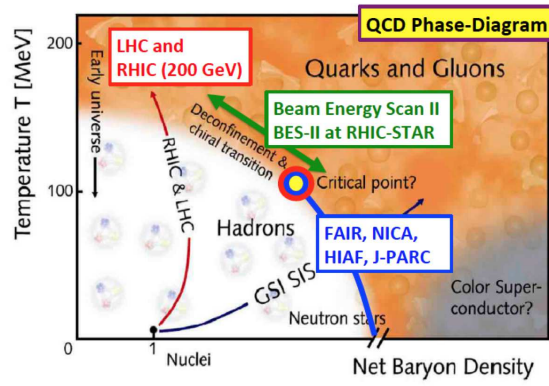
Figure 1: QCD phase diagram as a function of temperature and baryon density.

Figure 1 shows the QCD phase diagram with a possible location of the critical end point and a phase boundary of the first order phase transition. The properties of QGP and QCD phase transition at high temperature region have become more revealed with high beam energy collisions including more recent measurements from LHC experiments. Such a phase transition is shown to be a smooth crossover transition based on lattice QCD calculations. On the other hand, the detailed knowledge of QCD phase structure at high baryon density region still remains uncertain, especially the existence of the first order phase transition and the critical end point. The high baryon density region is expected to be accessible at relatively lower beam energy at RHIC. Therefore, RHIC beam energy scan phase-I program (BES-I) started in 2010 to study the QCD phase structure and to find the first order phase transition and the critical end point. Several hints of such signatures have been observed, which will be discussed in the following sections.

The RHIC beam energy scan phase-II program (BES-II) is under the way, aiming to confirm such hints with higher statistics and improved detector systems at STAR experiment and to finally explore details of the QCD phase structure at high density region. Figure 2 shows a schematic view of the main tracker TPC of the STAR detector and several detector upgrade projects for BES-II including (1) inner TPC read-out (iTPC), (2) end-cap Time-of-Flight (eTOF), (3) event plane detector (EPD), and (4) fixed target mode experimental setup (FXT). The BES-II program covers the beam energy region of 3 ∼ 30 GeV in $\sqrt{s_{NN}}$.
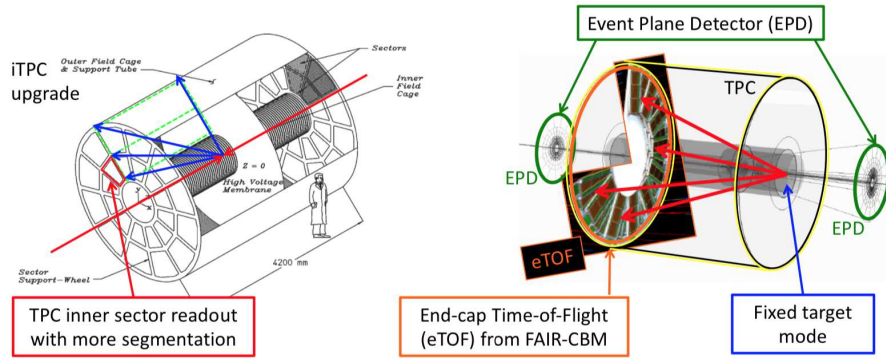
Figure 2: STAR detector upgrades for BES-II: inner TPC read-out (iTPC), end-cap Time-of-Flight (eTOF), event plane detector (EPD), and fixed target mode experimental setup (FXT).

## 2. Particle productions and freeze-out at high baryon density

One of the first steps of the beam energy scan program is to make sure whether the property of the matter created in the heavy-ion collisions has reached the higher density region of the QCD phase diagram. The left panel of figure 3 shows the results of chemical freeze-out temperature as a function of baryon chemical potential extracted by fitting the various identified hadron yields and ratios [1]. The extracted baryon chemical potential clearly shows the increasing trend with reducing colliding beam energy from 200 GeV down to 7.7 GeV in $\sqrt{s_{NN}}$, which indicates that the high baryon density matter has been created at least during the chemical freeze-out stage by scanning down the beam energy, that is mostly driven by increasing baryon stopping. The right panel of figure 3 shows the famous horn (a sharp peak-like) structure in K^+/π^+ ratio initially observed at SPS and later confirmed by the beam energy scan program at RHIC. This could be a signal from the phase transition, or explained by the associate production of Λ at high baryon density [2–5].
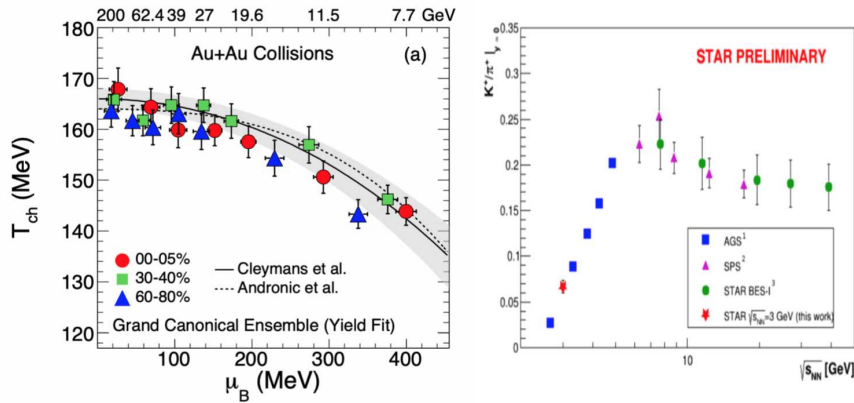
Figure 3: Chemical freeze-out parameters are shown on the left panel from the beam energy scan. K^+/π^+ ratio as a function of beam energy is shown on the right panel.

Hypernuclei ($^4_\Lambda H$ and $^3_\Lambda H$) yields at mid-rapidity are shown as a function of beam energy in the left panel of figure 4, where the new STAR measurements are taken with the fixed target

experimental mode at 3 GeV in $\sqrt{s_{NN}}$ and compared with various model predictions as well as the ALICE measurement at the LHC. The lifetime of these hypernuclei has also been measured and compared with various previous measurements in order to investigate possible differences to the free Λ lifetime. The directed flow v_1 of these hypernuclei are measured and the v_1 slope with respect to rapidity is plotted as a function of mass of the hypernuclei together with other light nuclei in the right panel of figure 4. The nucleon number scaling seems to hold, which indicates the nucleon coalescence as a dominant mechanism for the light nuclei production including the hypernuclei.
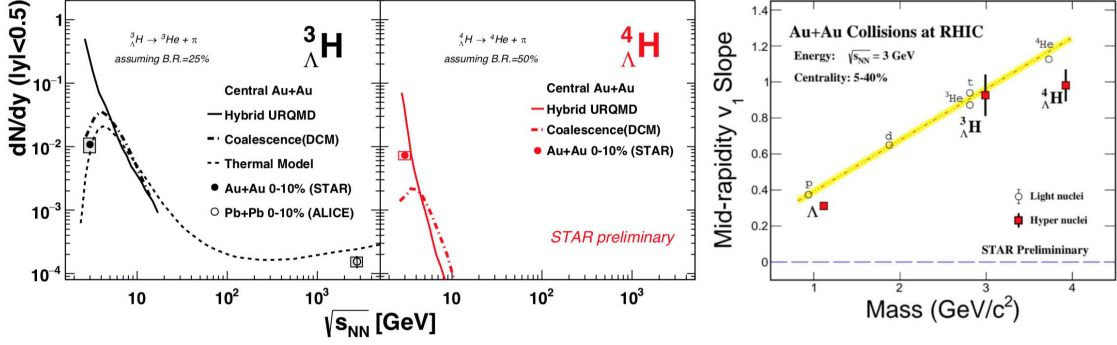
Figure 4: Hypernuclei ($^4_\Lambda H$ and $^3_\Lambda H$) yields as a function of colliding beam energy are shown on the left two panels. The directed flow v_1 slope at mid-rapidity as a function of nucleus mass is shown on the right panel.

3. Directed and elliptic flow

Collective flow is expected to encode the hydro-dynamic property of the quark and/or nuclear matter, where the radial flow could develop until the end of thermal freeze-out, while the azimuthal anisotropic flows are expected to be more sensitive to the earlier stage, because they are originated from the initial geometry. The directed flow v_1 is measured with respect to the first order event plane. The presented results are mostly v_1 odd contribution, that is anti-symmetric with respect to the rapidity, while v_1 even contribution has been minimized in the data analysis as much as possible.

The measured v_1 slopes as a function of collision energy are shown in figure 5 for various particle species in the left and top-right panels for hadrons and light nuclei, respectively [6–8]. The minimum and negative slope of net-baryon around 20 GeV might indicate a change in the property of quark-nuclear matter, that could be related to a softening of the equation of state and/or the first order phase transition. The bottom-right panel of figure 5 shows a typical trend of energy dependence of the elliptic flow v_2, which varies from the negative squeeze-out shadowing region to the positive pressure driven expanding region [8].

Figure 6 shows the transverse kinetic energy dependence of the elliptic flow v_2 of various hadrons after scaling both axes with the number of constituent quarks for each particle. The observation that the scaled v_2 falls onto a common curve for a given beam energy and centrality has been the major evidence of the partonic degree of freedom for the matter created at the RHIC and the LHC. This agreement seems to hold at higher beam energy region, while it starts showing some deviations at lower beam energy region especially at 3 GeV from fixed target mode experimental
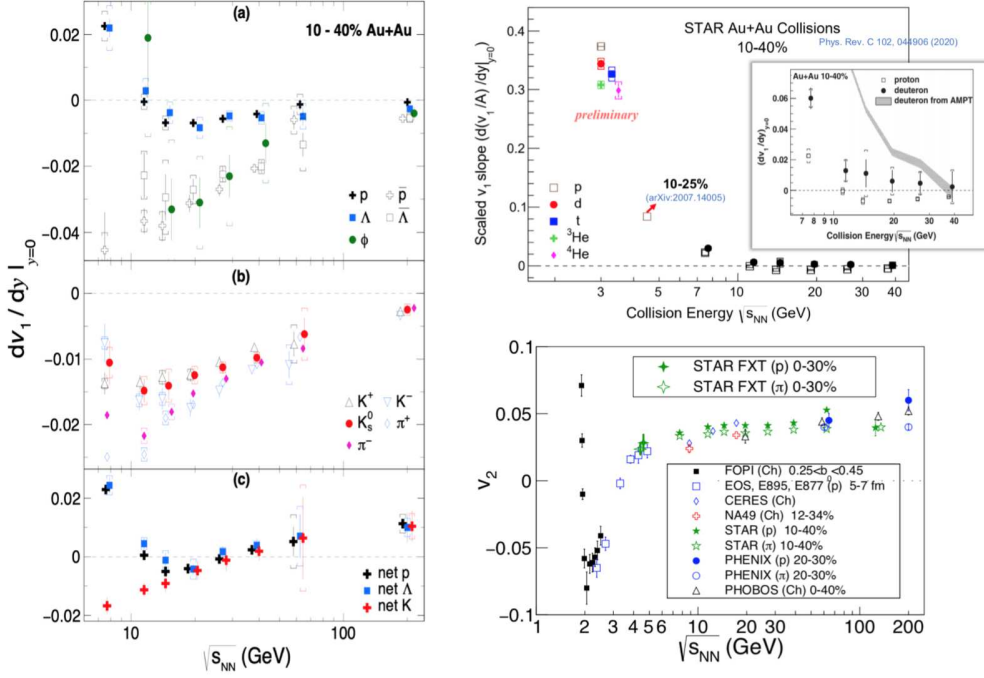
Figure 5: Energy dependence of directed flow v_1 and elliptic flow v_2 for various particle species.
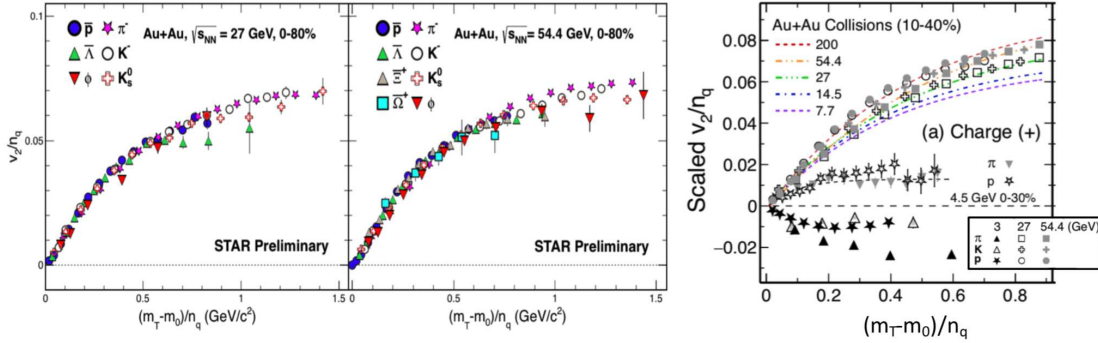

Figure 6: Number of quark scaled elliptic flow v_2 as a function of the quark number scaled $m_T - m_0$ for various particle species and colliding beam energies.

data, which is most likely driven by the hadronic system that has not entered the partonic phase during the evolution of these collisions [9].

4. High order net-proton fluctuations

The fluctuation of conserved number is expected to reflect a change in the correlation length of the high temperature and density system. It is also expected to diverge close to the critical end point and its sensitivity is supposed to be enhanced with increasing order of the cumulants. Experimentally, net-proton distribution is measured as a proxy of conserved net-baryon number

distribution. Ratios of the cumulants between different orders are shown in figure 7 as a function of beam energy, which is believed to be one of the most promising tools to look for a critical end point in the phase diagram. A hint of the non-monotonic behavior around 20 GeV and below, as seen in the 4th order cumulant ratio C_4/C_2 in panel (2), has been one of the driving forces of pursuing BES-II program at RHIC [10]. Looking for a deviation from the statistical Poisson baseline is the goal of current experimental measurements, which would include challenges to make experimental centrality resolution, initial volume fluctuation, their possible correlations as well as non-linear detector responses under control.
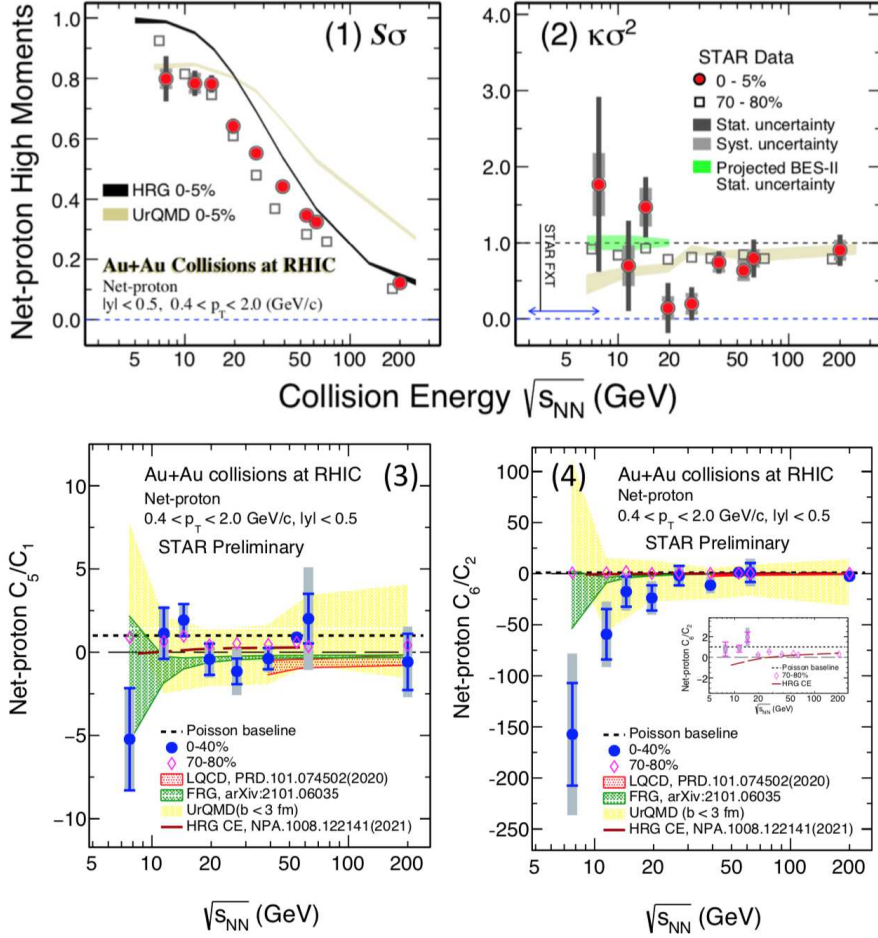
Figure 7: Ratios of high order cumulants of net-proton distributions, panel (1) for C_3/C_2, (2) C_4/C_2, (3) C_5/C_1, and (4) C_6/C_2, as a function of beam energy.

Figure 8 shows the cumulant ratios as a function of charged particle multiplicity at mid-rapidity from a small colliding system p+p to a large system Au+Au collisions at 200 GeV [11, 12]. This multiplicity is usually used to determine the centrality in heavy-ion collisions. For the net-proton fluctuation measurements, this charged particle multiplicity excludes proton and anti-proton in order to reduce the auto-correlation between cumulant measurements and centrality determination. The experimental data show a smooth transition from low to high multiplicity deviating from the statistical baseline at unity towards the central Au+Au collisions. The C_6/C_2 ratio changes from

positive in p+p collisions to negative in central Au+Au collisions, which is suggested as a possible signature of crossover phase transition by lattice QCD calculations.
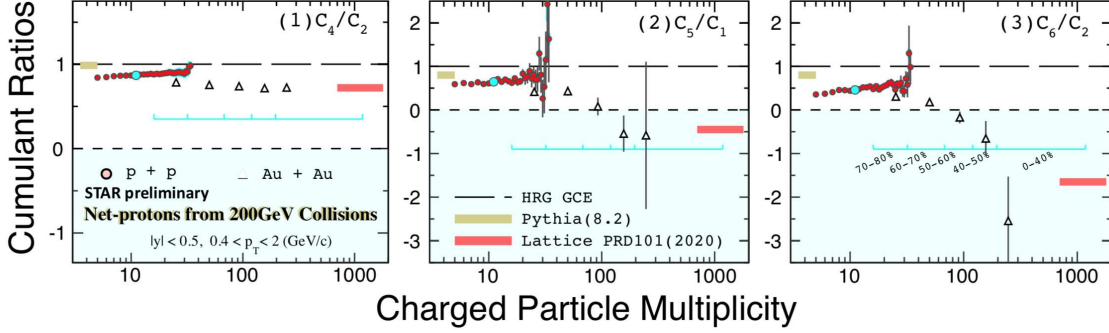

Figure 8: Ratios of high order cumulants of net-proton distribution, panel (1) for C_4/C_2, (2) C_5/C_1, and (3) C_6/C_2, as a function of multiplicity in p+p and Au+Au collisions at 200 GeV.

## 5. Femtoscopic HBT correlations

Results from 3-dimensional two pion quantum interferometry analysis [8] are presented in figure 9 including those from fixed target experimental mode in addition to the ones from the collider experimental mode. Correlations between sideward and longitudinal radius parameters are shown on the left panel, where each data point corresponds to one colliding beam energy from AGS to LHC. The geometrical shape of the source, which could be determined by the aspect ratio between transverse and longitudinal extents, might be quite different from a few GeV to a few TeV in $\sqrt{s_{NN}}$, while this could also be largely modified by the expansion dynamics in both transverse and longitudinal directions. The difference and ratio between two transverse radii along outward and sideward directions are expected to be related to the duration time of the colliding system, and are shown as a function of beam energy on the right panels of figure 9. A broad maximum has been observed around 20 GeV in $\sqrt{s_{NN}}$ which could result from the phase transition and/or critical point giving rise to a longer emitting source of the fire ball by a change/softening of the equation of state [13].

6. Chiral magnetic effect and global polarization

In non-central heavy-ion collisions, the motion of positively charged spectators as well as the angular momentum of the participant zone could induce a strong magnetic field perpendicular to the reaction plane, giving rise to the chiral magnetic effect (CME). The CME could be experimentally observed as charge asymmetries along the direction of the magnetic field or initial angular momentum direction. Earlier studies shown in the left panel of figure 10 exhibited a visible charge asymmetry signal especially in lower beam energy region at RHIC [14]. However, later investigations showed that a large fraction of the observed asymmetry could arise from other background effects. Therefore, data taking of two different isobar collisions (Ru+Ru, Zr+Zr), with the same
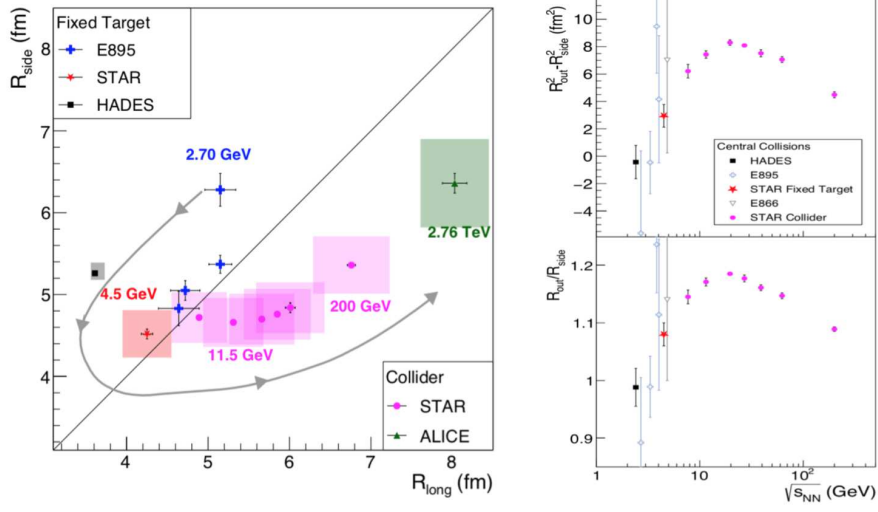
Figure 9: Extracted radius parameters from the 3-dimensional two pion HBT analysis: sideward and longitudinal radius correlation (left panel), difference and ratio between outward and sideward vs beam energy (right panels).
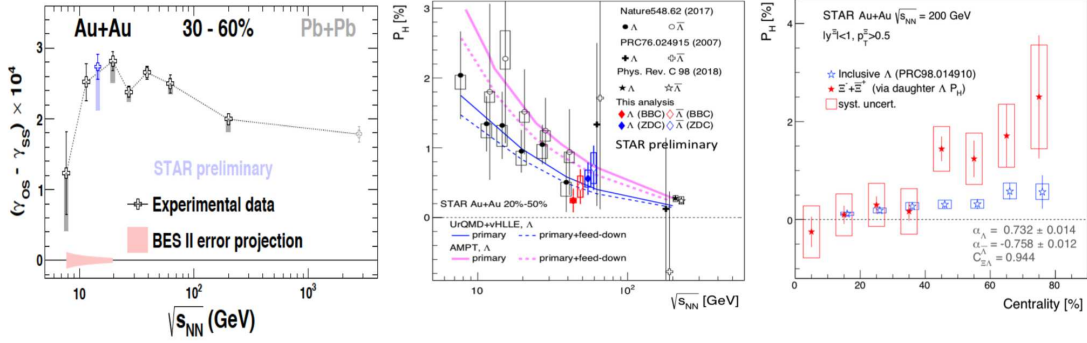

Figure 10: $\Delta\gamma$ difference between same and opposite sign charged pair correlation (left panel), global polarization of Λ, $\bar{\Lambda}$ (middle panel) as a function of beam energy, and centrality dependence of global polarization for Ξ and Λ (right panel).

mass number but 10 % difference in proton number, have taken place and a blind analysis procedure is being pursued in searching for the CME signal [15].

The strong vortical fluid in non-central heavy-ion collisions has been observed by measuring the hyperon polarization with respect to the angular momentum and/or magnetic field direction [16–18]. The observed global polarization is comparable between Λ and $\bar{\Lambda}$, which indicates this polarization is mostly given by the angular momentum of the system via spin-orbit coupling rather than the effect from the magnetic field. The magnetic field effect could still be non-zero, because of some remaining differences observed between Λ and $\bar{\Lambda}$. The global polarization has been found to show significant beam energy and centrality dependences, and there are some differences between different hyperons which could reflect the dynamical evolution of the colliding system [19].

7. Summary

Recent experimental results from the beam energy scan program at RHIC-STAR collaboration are presented. Their possible relations to the first order phase transition and the critical end point in the QCD phase diagram are discussed. The presented results include various particle productions including hypernuclei, freeze-out at high baryon density, directed and elliptic expansion, high order fluctuation of conserved number distribution, space and time structure from femtoscopic two-particle correlation, chiral magnetic effect and global polarization from expanding and vortical fluid as shown in above sections. Some of these measurements seem to indicate possible non-monotonic dependences and/or critical behaviors as a function of beam energy that we have been looking for. Ongoing and upcoming analyses of the BES-II data, more than 10-fold statistics than BES-I as shown in figure 11, would hopefully confirm the current measurements, answer remaining questions and open new directions.
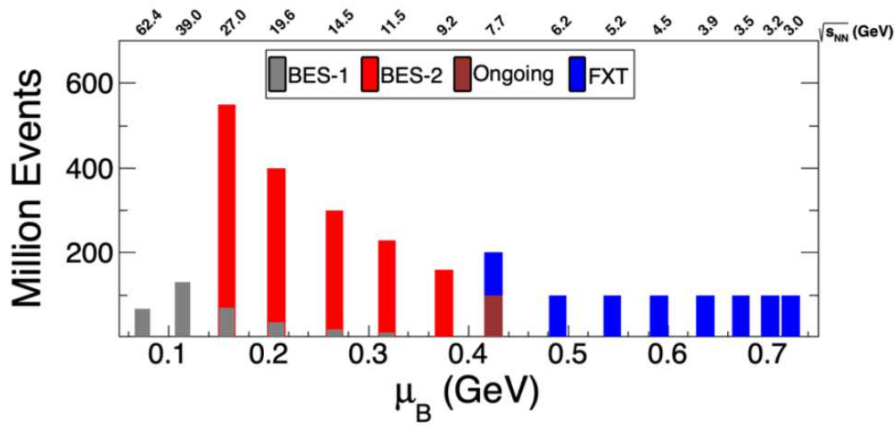
Figure 11: Expected statistics from the beam energy scan phase-II program including the fixed target experimental mode setup.

Acknowledgments

References

[1] STAR Collaboration, Phys. Rev. C 96 (2017) 044904, arXiv:1701.07065

[2] M. Gazdzicki, et al., Acta Phys. Polon. B30 (1999) 2705, arXiv:hep-ph/9803462

[3] J. Randrup, et al., Phys. Rev. C74 (2006) 047901, arXiv:hep-ph/0607065

[4] J. Rafelski, et al., J. Phys. G35 (2008) 044011, arXiv:0801.0588

[5] A. Andronic, et al., Phys. Lett. B673 (2009) 142–145, Phys. Lett. B678 (2009) 516, arXiv:0812.1186

[6] STAR Collaboration, Phys. Rev. Lett. 120 (2018) 062301, arXiv:1708.07132

[7] STAR Collaboration, Phys. Rev. C 102 (2020) 044906, arXiv:2007.04609

[8] STAR Collaboration, Phys. Rev. C 103 (2021) 034908, arXiv:2007.14005

[9] STAR Collaboration, arXiv:2108.00908

[10] STAR Collaboration, Phys. Rev. Lett. 126 (2021) 092301, arXiv:2001.02852

[11] STAR Collaboration, Phys. Rev. C 104 (2021) 24902, arXiv:2101.12413

[12] STAR Collaboration, arXiv:2105.14698

[13] R. Lacey, Phys. Rev. Lett. 114, (2015) 142301, arXiv:1512.09152

[14] STAR Collaboration, Phys. Rev. Lett. 113 (2014) 052302, arXiv:1404.1433

[15] STAR Collaboration, arXiv:2109.00131

[16] STAR Collaboration, Phys. Rev. C. 76 (2007) 024915, arXiv:0705.1691

[17] STAR Collaboration, Nature 548 (2017) 62, arXiv:1701.06657

[18] STAR Collaboration, Phys. Rev. C. 98 (2018) 014910, arXiv:1805.04400

[19] STAR Collaboration, Phys. Rev. Lett. 126 (2021) 162301, arXiv:2012.13601